Dimensional reduction by pressure in the magnetic framework material CuF₂(D₂O)₂(pyz): From spin-wave to spinon excitations

M. Skoulatos,[1,2] M. Månsson,[2,3,4] C. Fiolka,[5] K. W. Krämer,[5] J. Schefer,[2] J. S. White,[2,3] and Ch. Rüegg[2,6]

[1]*Heinz Maier-Leibnitz Zentrum (MLZ) and Physics Department E21, Technische Universität München, D-85748 Garching, Germany*
[2]*Laboratory for Neutron Scattering and Imaging, Paul Scherrer Institute, CH–5232 Villigen, Switzerland*
[3]*Laboratory for Quantum Magnetism, École Polytechnique Fédérale de Lausanne, Station 3, CH-1015 Lausanne, Switzerland*
[4]*Department of Materials and Nanophysics, KTH Royal Institute of Technology, SE-164 40 Kista, Sweden*
[5]*Department of Chemistry and Biochemistry, University of Bern, Freiestrasse 3, 3012 Bern, Switzerland*
[6]*Department of Quantum Matter Physics, University of Geneva, CH-1211 Geneva 4, Switzerland*

(Received 23 December 2016; revised manuscript received 14 July 2017; published 28 July 2017)

Metal organic magnets have enormous potential to host a variety of electronic and magnetic phases that originate from a strong interplay between the spin, orbital, and lattice degrees of freedom. We control this interplay in the quantum magnet CuF₂(D₂O)₂(pyz) by using high pressure to drive the system through structural and magnetic phase transitions. Using neutron scattering, we show that the low pressure state, which hosts a two-dimensional square lattice with spin-wave excitations and a dominant exchange coupling of 0.89 meV, transforms at high pressure into a one-dimensional spin chain hallmarked by a spinon continuum and a reduced exchange interaction of 0.43 meV. This direct microscopic observation of a magnetic dimensional crossover as a function of pressure opens up new possibilities for studying the evolution of fractionalised excitations in low-dimensional quantum magnets and eventually pressure-controlled metal–insulator transitions.

Interacting spin systems with strong quantum fluctuations are an indispensable platform for exploring concepts in quantum many-body theory. For rigorous tests of theory, it is often necessary to measure the system response due to external control parameters such as applied magnetic field and pressure (P). Just modest changes in these variables afford precise control over the strongly fluctuating degrees of freedom [1] and provide a direct route towards exotic physics such as magnetic field- and P-driven quantum phase transitions [2–4]. Another way to tune a system is to modify directly the magnetic superexchange, such as by changing the chemistry [5,6] or by generating a sizable *in situ* modification of the crystal lattice. While the latter case proves difficult to achieve, it is much sought-after since it promises the direct control of magnetic dimensionality. Moreover, such an *in situ* dimensionality change can be independent of the temperature, with such crossovers usually taking place as the density of thermal fluctuations varies.

The different topologies of one-dimensional (1D) and two-dimensional (2D) quantum spin systems are well-known to define strongly contrasting ground states and dynamics. In 1D systems such as the half-integer spin chain, fermionic fractional excitations termed unbound spinons give a characteristic excitation continuum that disperses only along the chain direction [7]. In contrast, on the 2D magnetic square lattice, Néel-order, and spin waves dispersing within the square lattice plane can be expected [8]. Exploring an *in situ* transformation between 1D and 2D magnetic regimes is experimentally challenging due to lack of suitable materials, but it can be expected to provide both a deeper understanding of the adjacent states, and potentially the discovery of unusual phenomena in the vicinity of the crossover. For example, in recent work on 2D magnetic square lattice systems such as Cu(DCOO)₂ · 4D₂O and La₂CuO₄, unusual features in the excitation spectra of each have been argued to reflect the existence of fractional excitations analogous to spinons in 1D systems [8,9]. Clarifying how fractional excitations evolve during a continuous 2D to 1D crossover can motivate new physical concepts, and at the same time provide links to related topics such as high-temperature superconductivity [10]. To progress the study of dimensional crossovers in quantum spin systems, simple materials with easily tunable structure-property relationships are required.

Here, neutron scattering has been used to explore a P-driven change of magnetic dimensionality in the metal organic compound CuF₂(D₂O)₂(pyz), where pyz = D₄-pyrazine (Fig. 1). At $P = 0$ kbar, and in agreement with a previous report [11], we find a simple antiferromagnetic (AFM) order below $T_N^{0\,\mathrm{kbar}} = 2.59$ K, where $S = 1/2$ moments of 0.6 μ_B/Cu²⁺ lie in the bc plane and are aligned along [0.7 0 1] in real space. With well-defined spin-wave modes dispersing along $(0, Q_k, Q_l)$ and no dispersion along Q_h, the system displays typical spin-wave dynamics of a 2D magnetic square lattice with $J_{2D}^{0\,\mathrm{kbar}} = 0.89(2)$ meV. Increasing P to 3.6 kbar leads to a slight reduction in T_N [$\Delta T = -0.13(1)$ K], and a small softening of the spin-wave modes [$J_{2D}^{3.6\,\mathrm{kbar}} = 0.78(3)$ meV]. Further increasing pressure to 6.1 kbar leads to an entirely new phase where both the magnetic order and spin-wave modes of the 2D state are completely suppressed. Instead, a spinon continuum is observed along the Q_h direction with $J_{1D}^{6.1\,\mathrm{kbar}} = 0.43(2)$ meV, which is the hallmark of a 1D spin chain. This remarkable P-driven magnetic dimensionality switch between 2D magnetic square lattice [Fig. 1(a)] and 1D spin chain [Fig. 1(b)] regimes is argued to be caused by a P-driven switch of a Jahn-Teller (JT) distortion characteristic to CuF₂(D₂O)₂(pyz).

At ambient P, CuF₂(D₂O)₂(pyz) has a monoclinic structure ($P2_1/c$) with cell parameters of $a = 7.6852$ Å, $b = 7.5543$ Å, $c = 6.8907$ Å, and $\beta = 111.25°$ at room temperature (RT) [Fig. 1(a)] [13]. The magnetic Cu²⁺ ions are coordinated by
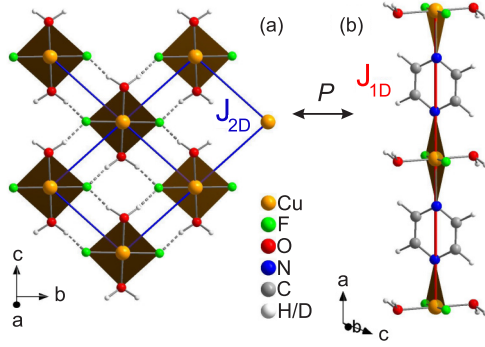
FIG. 1. $CuF_2(D_2O)_2$(pyz) crystal structure. (a) The α phase (ambient P) hosts 2D magnetic interactions on a slightly distorted square lattice. (b) The magnetic interactions switch to 1D in the β phase ($P = 6.1$ kbar). The brown rhombi denote the half-occupied magnetic orbital of Cu^{2+}.
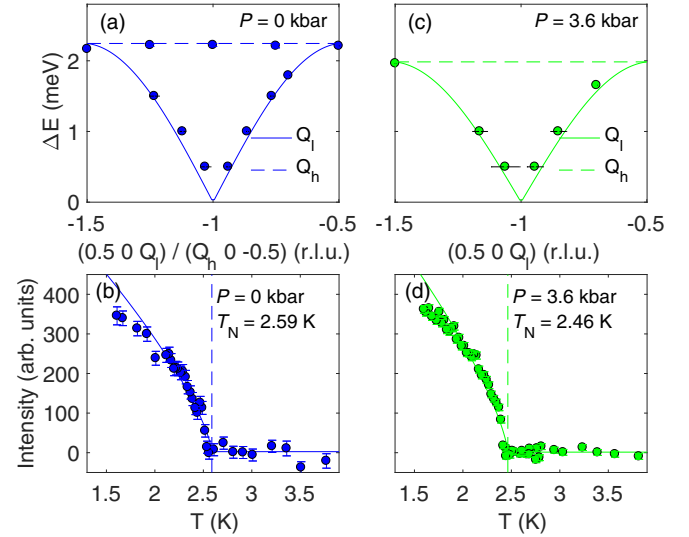

FIG. 2. Spin-wave excitations and magnetic order parameter of $CuF_2(D_2O)_2$(pyz) at $P = 0$ kbar [(a) and (b)] and at $P = 3.6$ kbar [(c) and (d)]. (a) and (c) show typical 2D spin-wave dispersions obtained at 1.5 K, with the data fitted using linear spin-wave theory. The solid (dashed) line are fits to the Q_l (Q_h) dispersion. (b) and (d) show the T dependence of the Bragg peak intensity at $\mathbf{Q} = (1/2\ 0\ 0)$, with a power-law fit for the low-T region (see text).

F^- ions, O (from D_2O), and N atoms (from pyz), all in *trans* positions of a slightly distorted octahedron with bond distances of Cu-F = 1.909 Å, Cu-O = 1.969 Å, and Cu-N = 2.397 Å. The Cu-F and Cu-O bonds are much shorter than the Cu-N bond, indicating that the half occupied magnetic $d_{x^2-y^2}$ orbital is localized in the bc plane and the elongated Jahn-Teller (JT) axis parallel to the a-axis [Fig. 1(a)]. Deuterium bonds (or hydrogen bonds in the nondeuterated form [12]) F$\cdots$D-O provide an efficient superexchange pathway between the Cu^{2+} ions and result in predominantly 2D magnetic interactions J_{2D} on a slightly distorted square lattice [13,14]. Importantly, the different Cu-X (X=F,N,O) bond lengths make the JT axis an additional and controllable degree of freedom [15].

Recently, $CuF_2(D_2O)_2$(pyz) was reported to show a series of P-driven, first-order structural phase transitions [13,16–18]. The ambient pressure phase, α-$CuF_2(D_2O)_2$(pyz), switches to β-$CuF_2(D_2O)_2$(pyz) at ~ 9 kbar, and γ-$CuF_2(D_2O)_2$(pyz) at $\sim$32 kbar. All of these phases exhibit the same crystal structure and maintain the monoclinic symmetry with space group $P2_1/c$. However, the elongated JT axis changes its orientation with increasing P from the Cu-N to the Cu-O and Cu-F bond for the α, β, and γ phases, respectively. β-$CuF_2(D_2O)_2$(pyz) has cell parameters of $a = 6.8607$ Å, $b = 7.6549$ Å, $c = 7.0904$ Å and $\beta = 114.289°$ at RT and 12.39 kbar [13]. The corresponding bond distances are Cu-F = 1.955 Å, Cu-O = 2.211 Å, and Cu-N = 2.019 Å. The elongated Cu-O bond locates the magnetic $d_{x^2-y^2}$ orbital in the ab plane. The Cu-F$\cdots$D-O-Cu superexchange paths in the bc plane are broken [Fig. 1(b)]. The switching of the JT axis results in a dramatic change of the magnetic properties between the α and β phases. While indeed bulk magnetic measurements indicate the α-β structural transition to separate very different magnetic regimes [13,17], direct microscopic characterization of the associated magnetic states has been lacking up to now.

Here, we report high-P neutron scattering studies of the microscopic magnetism in $CuF_2(D_2O)_2$(pyz) as pressure moves the system across the structural transition between the α and β phases. Our experiments were done using two single-crystal pieces of deuterated $CuF_2(D_2O)_2$(pyz) (total

mass 0.5 g) coaligned in the $(Q_h,0,Q_l)$ plane with a mosaic spread of $0.7°$. For high-P measurements, the sample was loaded inside a piston-cylinder clamp cell. The pressure transmitting medium was a 1:1 mix of fluorinerts FC-75:FC-77. The applied pressure was monitored *in situ* by tracking the lattice compression of a NaCl crystal co-mounted with the sample, and using its reported equation of state [19]. Inelastic neutron scattering (INS) data were collected using the TASP spectrometer at SINQ, PSI [20]. Fixed outgoing wave vectors $k_f = 1.3$ and 1.5 Å^{-1} were used, along with a Be filter placed between the sample and analyzer in order to suppress higher-order contamination. All INS data were collected at $T = 1.5$ K. Further neutron diffraction data were collected on the single-crystal diffractometer TriCS at SINQ, using $\lambda = 2.32$ Å.

Figure 2 shows a summary of the spin-wave dispersion and magnetic order in $CuF_2(D_2O)_2$(pyz) at $P = 0$ kbar [Figs. 2(a) and 2(b)] and at $P = 3.6$ kbar [Figs. 2(c) and 2(d)]. At $P = 0$, AFM long-range-order onsets below $T_N^{0\,\mathrm{kbar}} = 2.59(1)$ K [Fig. 2(b)]. The Néel temperature is suppressed at $P = 3.6$ kbar to $T_N^{3.6\,\mathrm{kbar}} = 2.46(1)$ K [Fig. 2(d)]. In both cases, the magnetic peak intensity has been fitted with a power-law behavior for the temperature range $T > 0.7 * T_N$ and with a mean-field critical exponent fixed to the 3D Heisenberg case [22].

The reduction of T_N by $\Delta T = -0.13(1)$ K upon increasing pressure is accompanied by a softening of the spin waves, as shown in Figs. 2(a) and 2(c). At both pressures, the magnetic excitations disperse away from the AFM Bragg point $\mathbf{Q} = (1/2\ 0\ -1)$, and along Q_l in the magnetic square lattice plane. In contrast, an essentially flat dispersion is observed along the out-of-plane direction Q_h. Figure 3 shows in detail some of the energy-transfer and Q scans used to construct the
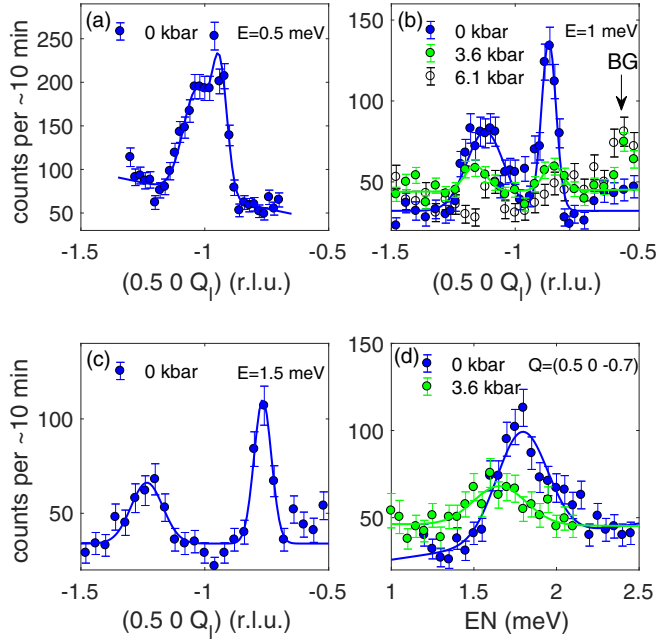
FIG. 3. INS data from $CuF_2(D_2O)_2(pyz)$ at all measured pressures and 1.5 K. (a)–(c) Q scans at 0.5, 1, and 1.5 meV energy transfers, respectively. (d) shows energy-transfer scans at $Q = (0.5 \ 0 -0.7)$. The sharp spin-wave modes completely disappear at $P = 6.1$ kbar [open points in (b)]. Gaussian fits are used throughout (solid lines). The feature denoted as "BG" in (b) for $P > 0$ is due to background from the pressure cell. It clearly disappears at $P = 0$, where the cell was not in use. Note that the data of 0 and 3.6 kbar belong to the same phase (square lattice) and this serves as an independent criterion for this background.

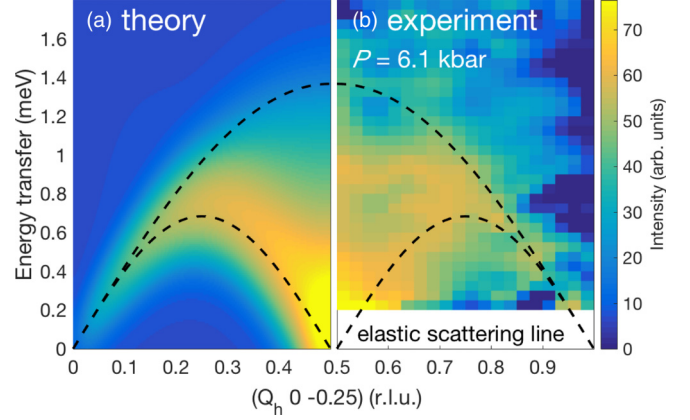FIG. 4. Magnetic INS intensity maps of the spectrum from $CuF_2(D_2O)_2(pyz)$ in the high-P phase. (a) shows the theoretical spinon dynamic structure factor [27]. (b) shows the experimentally measured spectrum constructed from individual energy-transfer scans equally spaced in Q. The dashed lines correspond to the lower and upper spinon boundaries according to the "des Cloizeaux-Pearson" analytical result [29].

dispersions shown in Fig. 2. Figures 3(a)–3(c) respectively show well-defined excitations in Q_l scans at fixed energy transfers 0.5 meV, 1 and 1.5 meV. Figure 3(d) shows energy scans at fixed $\mathbf{Q} = (0.5 \ 0 \ -0.7)$ for the two pressures. Here the shift down in energy of the peak at $P = 3.6$ kbar clearly shows a softening of the dispersion. A comparison between the two scans in Fig. 3(d) also shows a reduced signal-to-noise ratio [see also Fig. 3(b)], as a consequence of introducing the pressure cell.

Despite the slight softening of the excitation bandwidth at $P = 3.6$ kbar, the entire dispersion remains qualitatively similar. This strongly suggests α-$CuF_2(D_2O)_2(pyz)$ to host a regime of 2D magnetic interactions for all pressures in this structural phase. Using the SPINW library [23], we describe the dispersions using linear spin-wave theory [see Figs. 2(a) and 2(c)]. We find $\widetilde{J}_{2D}^{0\,kbar} = 1.05(2)$ meV and $\widetilde{J}_{2D}^{3.6\,kbar} = 0.92(3)$ meV for the 2D exchange coupling at each pressure, which become $J_{2D}^{0\,kbar} = 0.89(2)$ meV and $J_{2D}^{3.6\,kbar} = 0.78(3)$ meV after taking into account an appropriate quantum renormalization factor $Z_c = 1.18$ [11,21]. The result obtained at $P = 0$ kbar agrees well with previous work [11,17,18]. Using our results for J and T_N, we extract an empirical estimate [24] of the interlayer coupling $J_{\perp} \sim 3 \times 10^{-4}$ meV. This makes $CuF_2(D_2O)_2(pyz)$ an excellent realization of a 2D square lattice AFM.

At the highest $P = 6.1$ kbar, our $CuF_2(D_2O)_2(pyz)$ sample has transformed into the β phase [25]. In this phase at 1.5 K, we found no evidence for either magnetic long-range-order or any sharp magnetic inelastic modes. This evidences the suppression of the low-P 2D magnetic square lattice state, which has Q_k and Q_l as the main dispersion directions. Instead, fundamentally different behavior is observed, since the INS response is manifested as a continuum of broad-scattering modes that disperse only along Q_h, and have no Q_k or Q_l dependence. The experimental data are summarized as an intensity color plot in Fig. 4(b). The constituent energy scans used to construct Fig. 4(b), are shown in Fig. 5 [26]. From Figs. 5(a)–5(c) the dispersion along Q_h is clearly seen, while data in Fig. 5(d) show no significant dispersion along Q_l.

As can be seen in Fig. 4, the spectrum observed from $CuF_2(D_2O)_2(pyz)$ at $P = 6.1$ kbar [Fig. 4(b)] changes dramatically and compares well with that expected for a spinon continuum dispersion of a 1D spin chain [Fig. 4(a)] [27,28]. The good agreement between experiment and theory is further emphasized when (i) including the "des Cloizeaux-Pearson" analytical result [29], which defines the lower and upper spinon boundaries (dashed black lines in Fig. 4), and (ii) comparing the experimental data shown in Fig. 5, and the spinon intensities modelled using the formalism of Ref. [27] [continuous lines in Figs. 5(a)–5(c)]. From a simultaneous fit across all of our data, the spinon amplitude and J_{1D} parameters were refined, yielding $J_{1D}^{6.1\,kbar} = 0.43(2)$ meV. This lies in agreement with the value ~ 0.47 meV used in Ref. [17] to describe indirect bulk magnetization of the β-$CuF_2(D_2O)_2(pyz)$ phase. Overall, our results unambiguously unveil the high-P state of $CuF_2(D_2O)_2(pyz)$ to bear the hallmark magnetic response of a 1D spin chain.

Experimentally, we have observed a high-P 1D magnetic state to be present in β-$CuF_2(D_2O)_2(pyz)$ at $P = 6.1$ kbar. This pressure lies below ~ 9 kbar reported in Refs. [13,17] for the α-β structural phase transition, yet within the range of 5–15 kbar reported in Ref. [18]. A possible reason for any
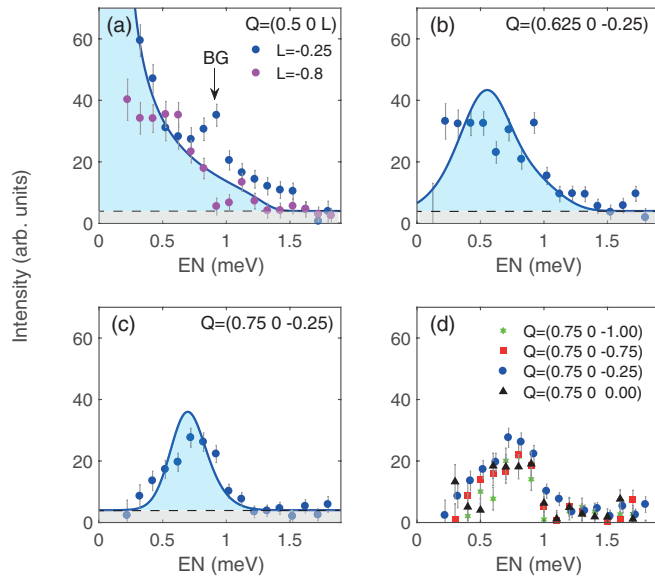
FIG. 5. Excitation spectra of $CuF_2(D_2O)_2$(pyz) in the 1D state. (a)–(c) show energy scans along the spin-chain direction Q_h. The solid lines are fits according to a theoretical spinon model [27]. (d) shows the spectrum to display no Q_l dependence. The scans in all panels are obtained after subtracting an energy scan at $Q_h = 0$ where no magnetic signal is expected (see Fig. 4). Despite this background subtraction, the signal denoted "BG" in (a) for $Q_L = -0.25$ is assigned to a parasitic, temperature-independent scattering process from the pressure cell as explained in the caption of Fig. 3. (a) includes an extra data set at a different Q_L value ($=-0.8$) with better conditions achieved, resulting to this background being absent.

absolute pressure variations across different studies can be due to the use of different methods of pressure generation and related inhomogeneities. Another factor that may be important is our use of deuterated $CuF_2(D_2O)_2$(pyz), since differences in properties could conceivably arise due to subtle changes between H and D bonding geometries [14,30]. While we cannot identify conclusively why the structural transition pressures vary between the different studies, we nevertheless observe directly a marked change in the system's magnetic and structural properties to occur over a pressure range that is broadly consistent with previous work [13,17,18].

A consistent understanding of the pressure-driven change between the low-P and high-P magnetic regimes is achieved if the JT axis of the $CuF_2O_2N_2$ octahedra switches from the Cu-N bonds [Fig. 1(a)] to the Cu-O bonds [Fig. 1(b)]. This switch leads to a reorientation of the $d_{x^2-y^2}$ orbitals from the bc plane at low-P to the ab plane at high P [13]. Without microscopic magnetic measurements, however, two competing scenarios for the high-P magnetic state could nevertheless be suggested: (i) the system in fact remains 2D, but with interactions in a different plane or (ii) 1D behavior arises if a particular exchange path dominates over all others. Our direct neutron scattering measurements reveal the existence of a spinon continuum [Figs. 4(b) and 5], confirming without doubt the 1D $S = 1/2$ spin chain to be the correct magnetic model for the high-P state.

Finally, we clarify the picture of the P-driven change in magnetic dimensionality in terms of the crucial exchange paths. In the 2D state, the Cu-F $\cdots$ D-O-Cu bonds define the superexchange pathways. To be effective at mediating superexchange for a 2D square lattice topology, the near-orthogonal superexchange integrals traversing the bc plane must be approximately equal. Once this bc-plane connectivity is suppressed, as happens in β-$CuF_2(D_2O)_2$(pyz) when the $d_{x^2-y^2}$ orbitals reorient to the ab plane, the 1D spin chain state suggests that strongest superexchange pathways become those that are linear along the Cu-pyz-Cu network [Fig. 1(b)]. In this case, the interaction J_{1D} along the Cu-pyz-Cu bond is expected to be of the σ type, and therefore weaker than for the 2D magnetic exchange in α-$CuF_2(D_2O)_2$(pyz). This picture is confirmed quantitatively from our data, since we find that $J_{1D}^{6.1\,kbar}/J_{2D}^{0\,kbar} \sim 0.5$.

In summary, our high-pressure neutron scattering study of the metal organic magnet $CuF_2(D_2O)_2$(pyz) unveils a dramatic P-driven switch of the system's magnetic dimensionality. From neutron scattering measurements of the magnetic excitations, we report that the 2D magnetic square lattice state at low-P transforms to a 1D spin chain at high P. The microscopic mechanism behind this behavior is argued to be a consequence of a P-driven switch of a uniquely sensitive Jahn-Teller axis in this soft material. Here lies the essence of this work: this JT switch across another direction, has a direct consequence on the orbital occupancies and in turn to the exchange pathways, which are completely altering the magnetism of the system in a profound way.

More generally, our work provides a reference example of how dramatic effects on the magnetic states in a 3D coordination material can be generated via modest perturbations [16,18,30,31]. Due to both the diverse range of metal organic materials with different ligands and networks that can be synthesized [32], and their generally higher compressibility compared with inorganic compounds, high P becomes *the* effective tool for seeking novel quantum states in these materials. In particular, the use of high P as a precision tuning parameter will be attractive for studying magnetic dimensionality changes across a *continuous P*-driven structure transition, as opposed to the first-order structural transition which takes place in $CuF_2(D_2O)_2$(pyz). In the former case, the coupling between strong quantum magnetic and enhanced structural fluctuations in the crossover region may lead to exotic quantum magnetic and magnetoelastic states [33,34]. An ultimate goal may also be to control a metal-insulator transition in such systems.

[1] *Introduction to Frustrated Magnetism*, edited by C. Lacroix, Ph. Mendels, and F. Mila (Springer, 2010).

[2] Ch. Rüegg, N. Cavadini, A. Furrer, H.-U. Güdel, K. Krämer, H. Mutka, A. Wildes, K. Habicht, and P. Vorderwisch, Nature (London) **423**, 62 (2003).

[3] S. E. Sebastian, N. Harrison, C. D. Batista, L. Balicas, M. Jaime, P. A. Sharma, N. Kawashima, and I. R. Fisher, Nature (London) **441**, 617 (2006).

[4] P. Merchant, B. Normand, K. W. Krämer, M. Boehm, D. F. McMorrow, and Ch. Rüegg, Nat. Phys. **10**, 373 (2014).

[5] M. Skoulatos, J. P. Goff, C. Geibel, E. E. Kaul, R. Nath, N. Shannon, B. Schmidt, A. P. Murani, P. P. Deen, and M. Enderle, Europhys. Lett. **88**, 57005 (2009).

[6] M. Skoulatos, J. P. Goff, N. Shannon, E. E. Kaul, C. Geibel, A. P. Murani, M. Enderle, and A. R. Wildes, J. Magn. Magn. Mater. **310**, 1257 (2007).

[7] D. A. Tennant, T. G. Perring, R. A. Cowley, and S. E. Nagler, Phys. Rev. Lett. **70**, 4003 (1993).

[8] B. Dalla Piazza, M. Mourigal, N. B. Christensen, G. J. Nilsen, P. Tregenna-Piggott, T. G. Perring, M. Enderle, D. F. McMorrow, D. A. Ivanov, and H. M Rønnow, Nat. Phys. **11**, 62 (2015).

[9] N. S. Headings, S. M. Hayden, R. Coldea, and T. G. Perring, Phys. Rev. Lett. **105**, 247001 (2010).

[10] G. Baskaran, Z. Zou, and P. W. Anderson, Solid State Commun. **63**, 973 (1987).

[11] C. H. Wang, M. D. Lumsden, R. S. Fishman, G. Ehlers, T. Hong, W. Tian, H. Cao, A. Podlesnyak, C. Dunmars, J. A. Schlueter, J. L. Manson, and A. D. Christianson, Phys. Rev. B **86**, 064439 (2012).

[12] In our experiments, we study the deuterated form of $CuF_2(D_2O)_2(pyz)$. The deuteration of hydrogen-containing compounds to be studied by neutron scattering is standardly done since it significantly reduces the incoherent neutron scattering. Consequently, for deuterated samples the background scattering detected is suppressed as compared with hydrogenated samples.

[13] G. J. Halder, K. W. Chapman, J. A. Schlueter, and J. L. Manson, Angew. Chem. Int. Ed. **50**, 419 (2011).

[14] P. A. Goddard, J. Singleton, C. Maitland, S. J. Blundell, T. Lancaster, P. J. Baker, R. D. McDonald, S. Cox, P. Sengupta, J. L. Manson, K. A. Funk, and J. A. Schlueter, Phys. Rev. B **78**, 052408 (2008).

[15] M. A. Halcrow, Chem. Soc. Rev. **42**, 1784 (2013).

[16] A. Prescimone, C. Morien, D. Allan, J. A. Schlueter, S. W. Tozer, J. L. Manson, S. Parsons, E. K. Brechin, and S. Hill, Angew. Chem., Int. Ed. **51**, 7490 (2012).

[17] S. Ghannadzadeh, J. S. Möller, P. A. Goddard, T. Lancaster, F. Xiao, S. J. Blundell, A. Maisuradze, R. Khasanov, J. L. Manson, S. W. Tozer, D. Graf, and J. A. Schlueter, Phys. Rev. B **87**, 241102(R) (2013).

[18] A. Lanza, C. Fiolka, M. Fisch, N. Casati, M. Skoulatos, C. Rüegg, K. W. Krämer, and P. Macchi, Chem. Commun. **50**, 14504 (2014).

[19] E. F. Skelton *et al.*, Rev. Sci. Inst. **55**, 849 (1984).

[20] F. Semadeni, B. Roessli, and P. Böni, Physica B **297**, 152 (2001).

[21] A. Pelissetto and E. Vicari, Phys. Rep. **368**, 549 (2002).

[22] J. Zinn-Justin, *Quantum Field Theory and Critical Phenomena* (Oxford University Press, New York, 1996).

[23] S. Toth and B. Lake, J. Phys.: Condens. Matter **27**, 166002 (2015).

[24] C. Yasuda, S. Todo, K. Hukushima, F. Alet, M. Keller, M. Troyer, and H. Takayama, Phys. Rev. Lett. **94**, 217201 (2005).

[25] From our neutron experiments at TASP and at $T = 1.5$ K, the crystal parameters accessible in the horizontal [$H0L$] plane were determined at each P (to accuracy 1 in the last digit). For $P = 0$: $a = 7.61$ Å, $c = 6.83$ Å, $\beta = 112.1°$, for $P = 3.6$ kbar: $a = 7.60$ Å, $c = 6.79$ Å, $\beta = 113.3°$, and for $P = 6.1$ kbar: $a = 6.87$ Å, $c = 7.09$ Å, $\beta = 113.4°$. The sharp change in a and c lattice parameters on going from $P = 3.6$ kbar to $P = 6.1$ kbar are consistent with the occurrence of the α-β structure transition, reported to take place at $\sim$9 kbar at RT [13,18].

[26] As a consequence of using the P cell, various reciprocal lattice Q_k, Q_l points were tested in terms of optimising the signal-to-noise for the measurements. The Q_h dependence was optimally conducted at $Q_k = 0$ and $Q_l = -0.25$.

[27] J.-S. Caux and R. Hagemans, J. Stat. Mech. (2006) P12013.

[28] M. Mourigal, M. Enderle, A. Klöpperpieper, J.-S. Caux, A. Stunault, and H. M. Rønnow, Nat. Phys. **9**, 435 (2013).

[29] J. des Cloizeaux and J. J. Pearson, Phys. Rev. **128**, 2131 (1962).

[30] K. R. O'Neal, T. V. Brinzari, J. B. Wright, C.-L. Ma, S. Giri, J. A. Schlueter, Q. Wang, P. Jena, and J. L. Musfeldt, Sci. Rep. **4**, 06054 (2014).

[31] P. A. Goddard, J. Singleton, P. Sengupta, R. D. McDonald, T. Lancaster, S. J. Blundell, F. L. Pratt, S. Cox, N. Harrison, and J. L. Manson, New J. Phys. **10**, 083025 (2008).

[32] C. P. Landee and M. M. Turnbull, Eur. J. Inorg. Chem. **2266**, (2013).

[33] *Handbook of Magnetic Materials*, edited by K. H. J. Buschow (Elsevier Science, Amsterdam, 2001).

[34] T. V. Brinzari, P. Chen, Q. C. Sun, J. Liu, L. C. Tung, Y. Wang, J. A. Schlueter, J. Singleton, J. L. Manson, M.-H. Whangbo, A. P. Litvinchuk, and J. L. Musfeldt, Phys. Rev. Lett. **110**, 237202 (2013).